

# Search for lost Point Sources using Mobile Gamma Spectrometry

**Master of Science Thesis**



Thomas Hjerpe  
Dept. of Radiation Physics  
The Jubileum Institute  
Lund University

Supervisors  
Christer Samuelsson  
Jacob Eberhardt

# Contents

<b>1. Introduction</b> .....	<b>1</b>
1.1 <i>Background</i> .....	1
1.2 <i>Aim of the work</i> .....	2
<b>2. Material and methods</b> .....	<b>3</b>
2.1 <i>The spectrometry system</i> .....	3
2.1.2 Carbone gamma spectrometry with GDM 40 RPS .....	4
2.2 <i>Theory</i> .....	5
2.2.1 The method for calculation of the detection limit .....	6
2.2.2 Spectrum .....	6
2.2.3 Statistical method; the <i>t</i> -test .....	7
2.3 <i>Data collection at Revingehed</i> .....	8
2.3.1 The detector .....	9
2.3.2 The source .....	10
2.3.3 Measuring procedure .....	11
<b>3. Results</b> .....	<b>13</b>
3.1 <i>Detection limits</i> .....	15
<b>4. Discussion</b> .....	<b>18</b>
4.1 <i>Geometry</i> .....	18
4.2 <i>The detection limit calculation method</i> .....	18
4.3 <i>Conclusions</i> .....	19
4.4 <i>Further studies</i> .....	19
<b>Acknowledgements</b> .....	<b>21</b>
<b>References</b> .....	<b>22</b>
<b>From raw data to results</b> .....	<b>23</b>
<b>Data on the <math>\mu</math>ACE<sup>TM</sup> amplifier and MCA card</b> .....	<b>26</b>

# 1. Introduction

## 1.1 Background

The use of mobile gamma spectrometry has over the years been used for various purposes. The activity concentrations of the natural radionuclides in rocks and soil have been measured for geological mapping and help in the search for mineral deposits, *e.g.* gold, tin and tungsten (*IAEA 1991*). Mapping of fallout and background radiation are two other applications (*Mellander 1988, IAEA 1991*).

Specially airborne gamma spectrometry, AGRS, has become a widely used tool in uranium exploration and mapping of fallout (*IAEA 1979*). AGRS was employed for mapping the fallout in Sweden after Tjernobyl (*Mellander 1988, SGAB 1990*).

The technique has also been used in the search for point sources. In January 1978 the Russian nuclear powered satellite Cosmos 954 disintegrated on re-entering the atmosphere in northern Canada. The radioactive debris was scattered over a large area, approximately 40 000 km<sup>2</sup>. Airborne gamma spectrometers (aircraft and helicopters) were used successfully in the search and recovery of the debris. The spectrometric procedure used was to study the ratio of low, 300-1400 keV, and high, 1400-2800 keV, gamma energies. The predominating gamma energies from the fission and neutron activated products lies in the low energy region stated above. So the main search technique was to look for increases in the low to high gamma energy ratio (*Grasty 1979, Bristow 1978*).

Another example of successful use of mobile gamma spectrometry is the recovery of a lost missile. In July 1970 a US Athena missile carrying two <sup>57</sup>Co sources, each of about 17 GBq, crashed in Mexico. Flying at an altitude of 75 m the count rate in a narrow <sup>57</sup>Co window was doubled when passing near the source. Then a ground recovery team was sent to the spotted location. The missile and the cobalt was found, unfortunately the sources were not intact; the activity was distributed over a relatively large area (*Deal et al 1972*).

Both operations above used the spectrometer mounted in an aircraft. The possibilities and problems with airborne gamma spectrometry has been well investigated (*IAEA 1991*). The main effort in this field of research has, as said earlier, been to develop methods for measuring surface activity and fallout or searching for

minerals. Lately the interest in methods for finding lost point sources have increased, specially after the fall of the Berlin wall and the collapse of the Soviet union. The risk of smuggling radioactive material can not be neglected. Another reason for the need of research in searching for point sources is the amount of transportations with radioactive material. Every year 100000 packages of radioactive goods are transported in Sweden; about a tenth of them has an activity over 10 MBq (*Finck, 1996*).

## **1.2 Aim of the work**

The purpose of this work is to test a method for locating lost point sources in the environment with carborne gamma spectrometry and study different geometries for the detector. The use of a car is chosen because it is inexpensive and easy to handle compared to airborne methods, there are no need for pilots and airports. The disadvantages of a car, compared to an aircraft, are the slow speed and the restriction to roads or other roadworthy areas. These disadvantages, however, are partly compensated for; the probability should be greatest when something is lost, or dumped, that it is located near a road.

This thesis is the beginning of a larger project in mobile gamma spectrometry. One goal is to develop reliable and sensitive on-line methods for finding lost point sources; on-line means that the results are presented direct in the field without the need for further analysis back home in the laboratory.

The scope of this thesis has been limited to first investigate how far away from a road a strong  $^{137}\text{Cs}$  source can be detected with a certain analysis method at different speeds and detector geometries. Second, suggestions for further investigations will be presented.

## 2. Material and methods

### 2.1 The spectrometry system

Gammadata AB, in Uppsala, was commissioned by the Swedish Radiation Protection Institute, SSI, to construct a system for mobile gamma spectrometry.

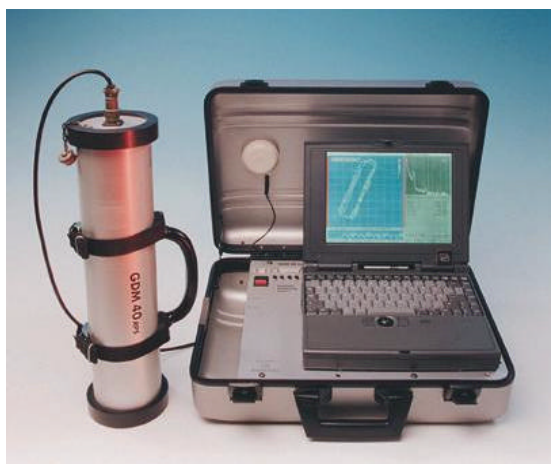


*Fig 2.1.* The GDM 40 RPS system for mobile gamma spectrometry. The tube on the left is the 3"x3" NaI-detector.

The system, named GDM 40 RPS (se fig 2.1), includes:

- Microprocessor control board (Gammadata)
- Multichannel analyser, MCA (EG&Ortec,  $\mu$ ACE™)
- NaI detector (Teledyne, 3"x3")
- Photomultiplier (EG&Ortec, ScintiPack™, 296 tubes)
- GPS (Trimble Navigation 6 channel GPS sensor)
- DGPS

The microprocessor controls the MCA and transfer data between the MCA<sup>1</sup> and the GPS unit. GPS, Global Positioning System, is a satellite based positioning system developed by the US military for determination of exact locations world-wide. In 1993 the system was completed and consists of 26 NAVSTAR satellites (24 operative and 2 spare satellites in case of failure) in six different orbits; this results in 24-hour coverage of all the earth's surface with 6-7 satellites visible at all times. The satellites transmit

---

<sup>1</sup> See Appendix B for data on the MCA

there exact location and elevation, the GPS receiver can then determine its location on the earth's surface when it sees three satellites or more (with four satellites the location and altitude can be determined). In the standard GPS, available to the public, the signal from the satellites is slightly altered to decrease the accuracy of the positioning; the error in the position is about 50 m. DPGS, Differential GPS, is a method of decreasing this error. The principle is to use land based beacons that transmit there exact position to an optional receiver attached to the GPS unit. The accuracy of the positioning can then be down to 10 cm; however higher accuracy increases the costs. The system used here is equipped with a DGPS that has an accuracy of about 10 m which is enough for this purpose.

A portable PC, Hewlett Packard Omnibook 600C, is also connected to the system. The DOS based software for spectrometric analysis is developed and written by Hans Mellander, SSI.

The whole system, except for the detector, is mounted in an attaché case of aluminium, which make it portable; one of the manufactured systems is actually mounted on a backpack. This thesis concerns carborne methods so the use of a bigger, more sensitive, detector is possible. At the department of radiation physics in Lund, there was recently a change of the crystal in the whole body counter, and the old one was available. The old crystal, 8"x4" NaI(Tl), was then used in this project. This bigger crystal gives about 5 times higher countrate in the Cs window compared to the 3"x3" crystal which is an advantage.

### **2.1.2 Carborne gamma spectrometry with GDM 40 RPS**

The system works as a common multi channel spectrum analyser, with one additional feature; each spectrum is assigned a geographical co-ordinate by the GPS. The sampling time of a spectrum should be long enough to get adequate statistic, but short enough to get good spatial resolution. A sampling time between 1 and 10 s is common, depending on the sensitivity of the crystal. A sampling time of 5 s for the 8"x4" crystal was chosen throughout this work. Thus, if the car is driving at a speed of 20 m/s a new spectrum is sampled at every 100 m. Below is an example of results from carborne gamma spectrometry with the GDM 40 RPS system.

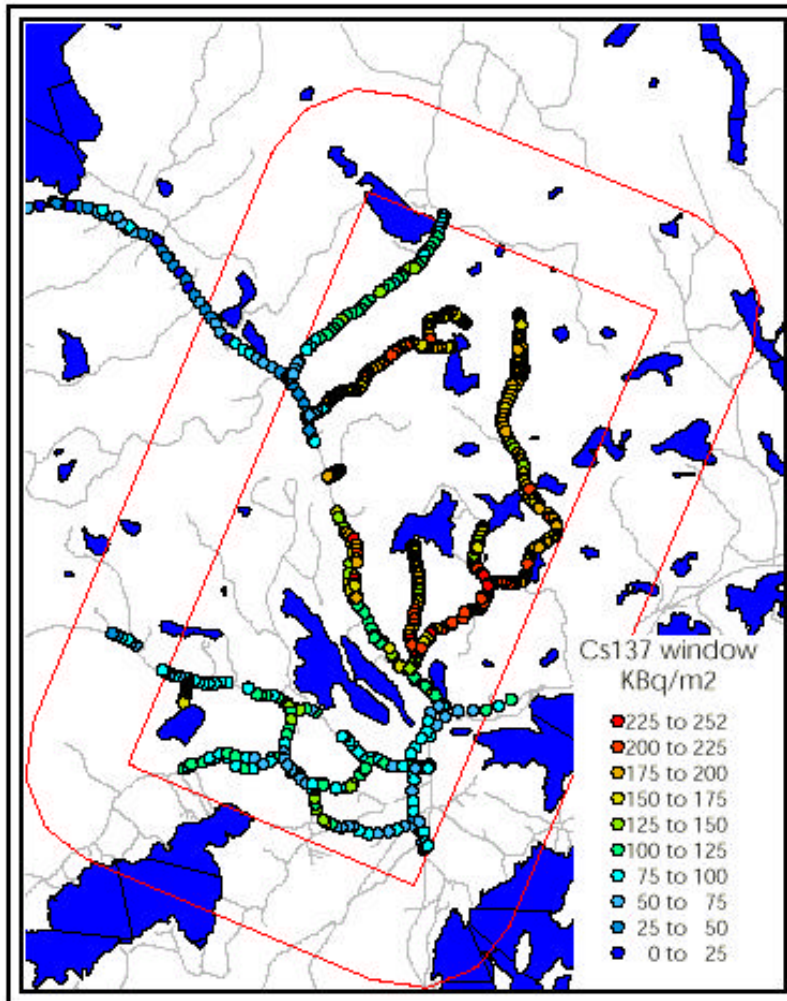


**Fig 2.2.** This picture shows how the data can be presented with the GDM 40 RPS system. In August 1995 the Nordic Nuclear Safety Project arranged an exercise in Finland. The main object was to compare results from different measurement systems. Each circle represents the contents of <sup>137</sup>Cs in one spectrum, based on a colour scale. (Samuelsson, Eberhardt unpublished).

## 2.2 Theory

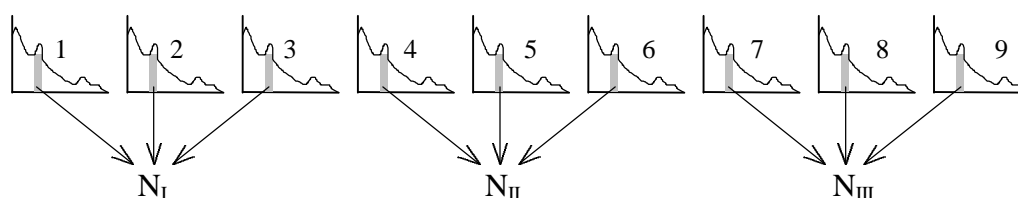
The aim of the analysis is to determine the *detection limit*. The detection limit is defined as: the longest distance from the road that the source can be detected with sufficient statistic significance; this level is up to the user to choose, depending on how many false alarms that is acceptable.

To determine the detection limit a combined experimental and theoretical approach was taken. Field measurements with the source placed at different distances from the road and the car standing still on different locations on the road was studied. Theoretical studies of the spectra for different speeds of the car from the stationary obtained spectra were performed.

In the calculations of the detection limit, total counts in the <sup>137</sup>Cs windows was the chosen parameter.

### 2.2.1 The method for calculation of the detection limit.

The method compares nine in time consecutive spectra. The mean of the total counts in the  $^{137}\text{Cs}$  window (500 to 800 keV) for the three spectra in the middle is compared to the mean of the counts for the six surrounding spectra. Schematic it can be explained:



$N_{II}$  is then compared to  $\frac{1}{2}(N_I+N_{III})$

**Fig 2.3.**

If  $N_{II}$  is higher than  $\frac{1}{2}(N_I+N_{III})$ , with a chosen significance level, the test gives alarm. The test used for evaluating the significance, the  $t$ -test, is explained below. Each analysis consists of information from nine spectra, *i.e.* it corresponds to quite a distance driven on the road; *e.g.* 625 m if the speed is 50 km/h. The co-ordinate given to each test is the co-ordinate for the fifth spectra, the one in the middle.

The advantages of this method are that it is insensitive against slow variations in the background, fairly insensitive against rapid changes in the background and easy to apply on-line; the disadvantage is that it favours situations where the source only can be seen in three or less spectra.

### 2.2.2 Spectrum

The spectra to be evaluated were obtained at different times, sometimes days apart. During that time the drift in the electronics can cause considerable differences in the channel width of the spectrum; from 10 to 14 keV/channel were obtained. To get comparable spectra when calculating the detection limit some modifications were performed<sup>2</sup>. First all spectra were energy calibrated and then transformed to the same channel width, 12.5 keV/channel. The gain was set so the energy range spanned from 0 to 3000 keV, approximately.

---

<sup>2</sup> See Appendix A for details

### 2.2.3 Statistical method; the $t$ -test

The test used for determine if the mean of the three spectra in the middle differ from the surrounding spectra is a common test in mathematical statistic, the  $t$ -test. This test is often used when the number of samples are small, here we have means of 3 and 6 values respectively. The formula used have several slightly different variations, depending on the conditions. In this case the conditions are:

- The quantities to compare are both means
- We are only interested in positive signs, *i.e.* when  $N_{II}$  is greater then  $\frac{1}{2}(N_{III}-N_I)$
- The population standard deviations of the means are not always comparable in size

The first condition leads to the use of a two-sample test, the second to the use of a single-sided test. The third condition cause problems in the  $t$ -test when the population standard deviations of the two means not are of comparable in size, *i.e.* when the point source contribute to a great number of pulses in some of the spectra. To avoid this problem a transformation of the data are performed before applying the test; the choice of transformation of the data depends on the behaviour of the standard deviations. Here we have standard deviations that are proportional in size to the square root of the means, if we make the assumption that the number of pulses in the Cs window are Poisson distributed. The data was therefor transformed by taking the square root of every value before performing the test, ( $v=\sqrt{N}$ ). The one-sided two-sample  $t$ -test designed for small samples and equal standard deviations can then be used. The wanted test statistic,  $t$ , then is calculated with the following expression:

$$t = \frac{\bar{n}_1 - \bar{n}_2}{s\sqrt{\frac{1}{m_1} + \frac{1}{m_2}}} \quad s = \sqrt{\left[ \frac{(m_1 - 1)s_1^2 + (m_2 - 1)s_2^2}{(m_1 + m_2 + 1)} \right]} \quad (2.1) \ \& \ (2.2)$$

- $\bar{n}_1$  is the transformed mean of the three middle spectra, *i.e.*  
 $\frac{1}{3}[\sqrt{N_4} + \sqrt{N_5} + \sqrt{N_6}]$ ,  $N_i$  is the counts in the Cs window for spectrum  $i$ .
- $\bar{n}_2$  is the transformed mean of the surrounding spectra.

$m_1$  and  $m_2$  are the number of measurements contributing to  $\bar{n}_1$  and  $\bar{n}_2$ .  
respectively, *i.e.* three and six.

$s_1$  and  $s_2$  are the estimated standard deviation of the two samples. Also  
calculated

with the transformed values

$s$  is the combined estimation of  $s_1$  and  $s_2$ .

$m_1+m_2+1$  is the degrees of freedom, *d.f.*

The estimated standard deviations for the samples,  $s_1$  and  $s_2$ , are calculated as the Poisson standard deviation of the transformed number of pulses,  $\sqrt{N_i}$ . For example:

$$s_1 = \frac{1}{3} \left( \sqrt[4]{N_4} + \sqrt[4]{N_5} + \sqrt[4]{N_6} \right) \quad (2.3)$$

The possibility,  $P$ , that  $\bar{n}_1$  is significant greater than  $\bar{n}_2$  is then read out from Student's single-sided  $t$  distribution.

$$P = f(t, d.f.) \quad (2.4)$$

$P$  is the quantity that determines the detection limit; if  $P$  is greater than the by the user chosen percentage, the test indicates that the system found a source. The lower  $P$  is chosen the greater becomes the risk for false alarms, but the detection limit is increased.

### 2.3 Data collection at Revingehed

The practical measurements were performed with the above described system, equipped with the 8" NaI crystal, mounted in a GMC Van.

SSI in Stockholm provided a 6 GBq  $^{137}\text{Cs}$  for the practical measurements; these were performed in the military training ground at Revingehed. The advantages with Revingehed were the flatness of the field, *i.e.* the source could radiate in a  $2\pi$  geometry, and that there were very few people in the area, which was beneficial from a radiation protection point of view.

In the evaluation of the data, the methods used can be divided into two main groups:

- methods with subtraction of natural and cosmic background radiation
- methods with no subtraction of natural and cosmic background radiation

The ideal situation would be to have a subtraction method that always corrects for the accurate background, *i.e.* the net spectra would be zero in all channels unless a source is present. This method does not exist in practice due to the stochastic nature of radiation. When searching for point sources in areas with reasonably stable background, there is no need for correction; the goal is just to find the source so a relative measurement is enough. If the search is performed in areas with large variations in the geological surroundings, the need for background subtractions might be justified; for example in areas with alternating rock faces, lakes and forest. The approach with no background corrections is used in this report; the measurements were performed in an area with very low and stable background.

In both methods above the spectra must be energy calibrated. Thus, the method in this report uses spectra that are energy calibrated but not corrected for the natural or cosmic background.

### **2.3.1 The detector**

The placement of the detector in the car is important for the result. The possibility that something screens off the source from the detector increases with decreasing detector-ground distance. Therefore the detector was placed as high as possible inside the car; the detector-ground distance then became about 2 meters. Another advantage with high placement in the car is that the detector does not come so near the wheel housings, which is favourable in areas with fresh fallout; the wheel housings can then be contaminated. The problem with contaminated wheel housings is a greater problem when measuring ground concentrations of radionuclides, especially direct after fallout. To further decrease the influence of the car on the spectra the detector was placed near the back of the car and partially surrounded by shielding material.

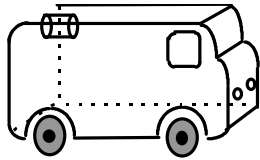


**Fig 2.4.** Placement of the detector in the car  
(cylinder = detector)

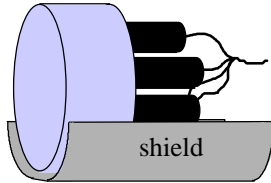


**Fig 2.5.** The detector shielding

The shield was made of 12 mm lead and a thin copper sheet, the purpose of the copper was to attenuate characteristic x-rays from the lead.

Next question was, how should the detector be directed in the car? Two directions were investigated:

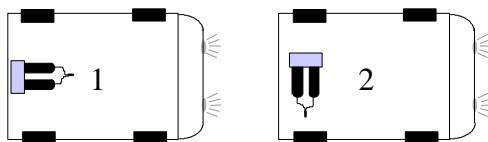


**Fig 2.6.** Detector directions in the car:

1. backwards
2. sideways

The purpose with the backward geometry is to get symmetrical sensitivity for finding the source, *i.e.* it does not matter on which side of the road the source is located. The second geometry is more sensitive at one of the sides of the road.

One disadvantage with the 8" crystal is that it can not be powered by the internal power supply in the GDM 40 RPS system; therefore an external power supply and high voltage module were used<sup>3</sup>. In the car 220 V is available so the system can still be mobile.

### 2.3.2 The source

Two small steel cylinders containing  $^{137}\text{Cs}$ , 3 GBq each, were used. Handling this amount of activity demands a strategy when working with it to keep the personal dose down. Every high dose rate step were first trained with blind sources and distance tools were used as much as possible.

<sup>3</sup> Tennelec Minibin, TennelecTC909 (power supply), Canberra3102D (HV), Canberra2005 (pre-amp.)

The sources were placed in a plastic test tube and put in a lead container on a cart; the sources could then be safely transported out in the field. The test tube was connected to a string; an arrangement was made so the test tube could be pulled up from the lead container, after the lid was opened, and fixed ten centimetres above the container. The nearest part of the body (the hands) then had a distance of about one meter to the sources, so this arrangement was beneficial from a radiation protection point of view. When the source was in “*radiating mode*”, *i.e.* pulled up from the container, it was about half a meter above ground and radiated in all directions, except for straight backwards where the lid of the container was shielding. The back scatter contribution to the  $^{137}\text{Cs}$  window from the lid can be neglected.



**Fig 2.7.** The cart with the source in “radiation mode”.

This device kept the personal dose at reasonably a low level, approximately  $50 \mu\text{Sv}$  excluding background, during the two months of field measurements.

### 2.3.3 Measuring procedure

The normal way to do mobile gamma spectrometry is to drive and measure at the same time. At Revingehed another approach was taken; stationary measurements were performed 25 m apart on the road. From these spectra the count rate in the Cs window were interpolated for every 5 meters. The counts in the Cs window in a real measurement with arbitrary speed, sampling time and position on the road can then be estimated<sup>4</sup>, which is the advantage with this method. Because the final goal, which is

---

<sup>4</sup> See Appendix A for details

beyond this report, is to optimise methods for finding point sources the optimum speed and sampling time is yet not known. Thus by using this approach no calculations have to be done in advance to decide what speeds and sampling times that should be measured in the field.

A co-ordinate system was assigned to the road; origo was placed at the point where the source was closest to the road. The source was placed at different distances,  $a$ , from the road.

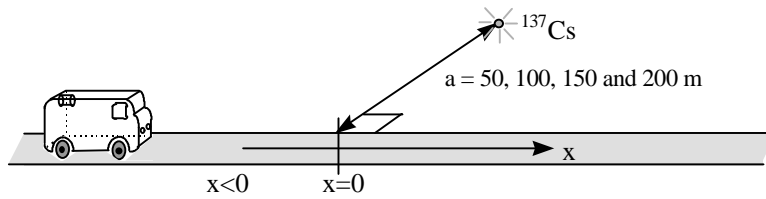
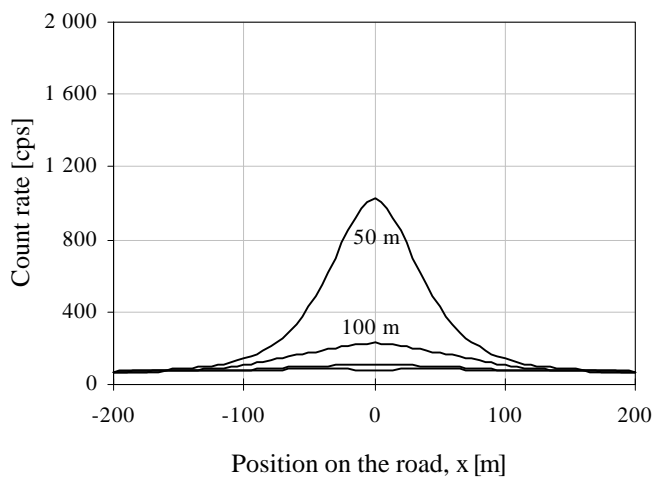


**Fig 2.8.** The co-ordinate system on the road and the used source to road distances,  $a$ .

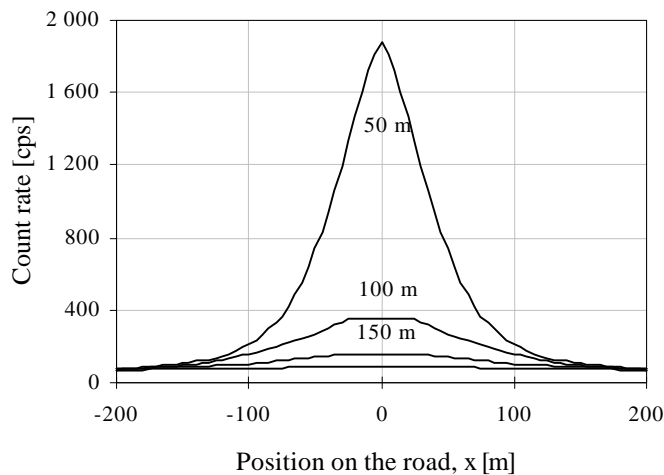
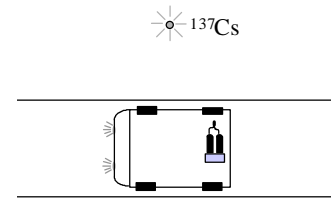
Each spectrum is assigned the  $x$  co-ordinate that corresponds to the point where the detector is located at the time when half the spectrum is collected, *i.e.* after 2.5 s (the sampling time used was always 5 s).

### 3. Results

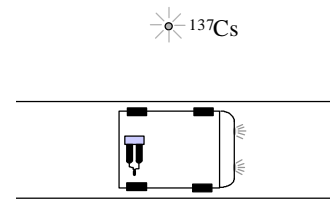
After the interpolations, the count rates every 5 meters for the different source-road distances were obtained. When directing the detector sideways two different situations can occur depending on which side on the road the source is lying: the crystal facing the source, *i.e.* the source is lying on “the right side” or the PM-tubes facing the source, *i.e.* the source is lying on “the wrong side”. When directing the detector backwards, the count rate is independent on which side of the road the source is located. This means that three different count rates were calculated, se figure below.



Detector pointed sideways  
Source on "the wrong side"



Detector pointed sideways  
Source on "the right side"



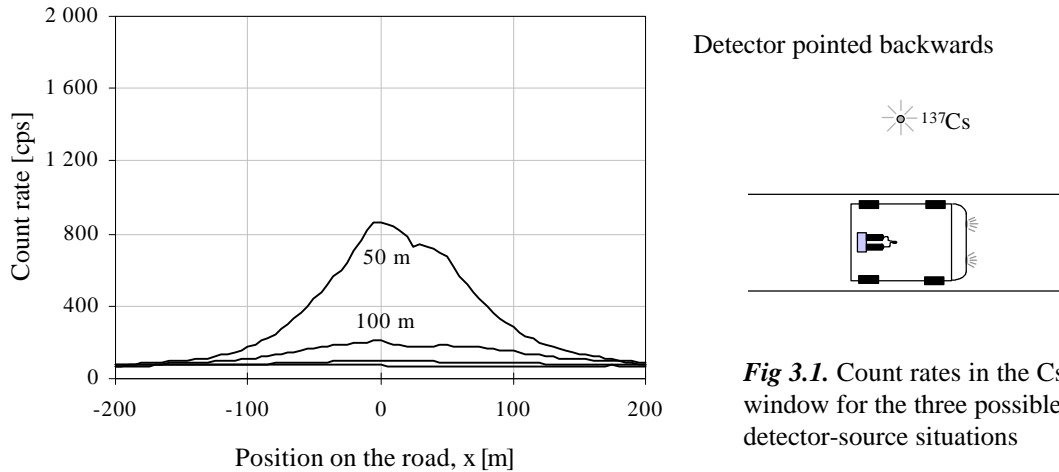


**Fig 3.1.** Count rates in the Cs window for the three possible detector-source situations

In the graphs above it is indicated that the sensitivity of the detector depends on the directions of the crystal. There is a factor two difference in the maximum count rate between the two situations. This difference is due to the fact that the intrinsic efficiency of 660 keV photons is nearly 100 % from both directions which means that the absolute efficiency is proportional to projected area of the crystal (*Knoll 1989*); the area projection is roughly a 1.5 times bigger from the front of the crystal than from the side. There is also an additional decrease in the count rate in the “backward” geometry due to the lead shielding, se figure 2.5, that explains the rest of the difference in count rate.

Another important notation from the graphs above is that the count rate in the backward geometry and the sideways geometry that have the PM-tubes between the source and detector not differ so much, just about 10 percent.

The last remark about the graphs in figure 3.1 concerns the shape of the curves. The two first, the sideward geometries, both have curves that are symmetrical about origo, while the third curve, the backward geometry, has higher count rates at positive x coordinates. This effect is caused by the lead shielding; after the car has passed the source, the shielding do not longer come in the way for the primary photons from the source.

The resulting count rates in figure 3.1 were used to calculate expected results from real measurements with a moving car; the procedure for this is discussed in detail in appendix A. Total number of counts, *i.e.* with background, in the Cs window for three

different speeds were simulated, 32, 54 and 68 km/h, for the four source-road distances in figure 2.8.

The spectra then covers following range on the road:

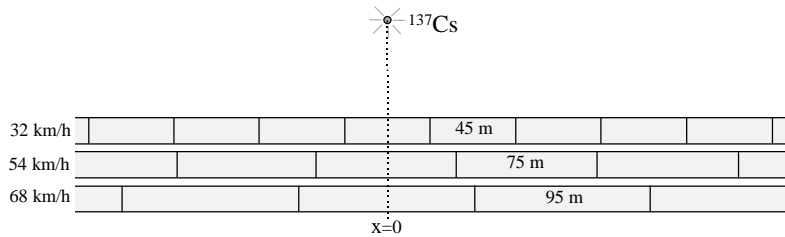


**Fig 3.2.** The part of the road the spectra covers at different speeds and the spatial length of the spectra.

The spectra were constructed so one spectrum became symmetrical about  $x=0$ , *i.e.* the point on the road where the Cs was closest to the road. This is the ideal situation, the spectrum obtained closest to the source contains as many photons from the Cs as possible.

### 3.1 Detection limits

How the detection limit was calculated from the constructed spectra will be discussed below for the backward geometry at the simulated speed of 32 km/h, for the other speeds and geometries only the result will be presented.

The counts in the in the Cs window for one of the source-road distances, 100 m, as function of the position on the road, the position is set to when half the spectrum is collected (after 2.5 s), is plotted below.

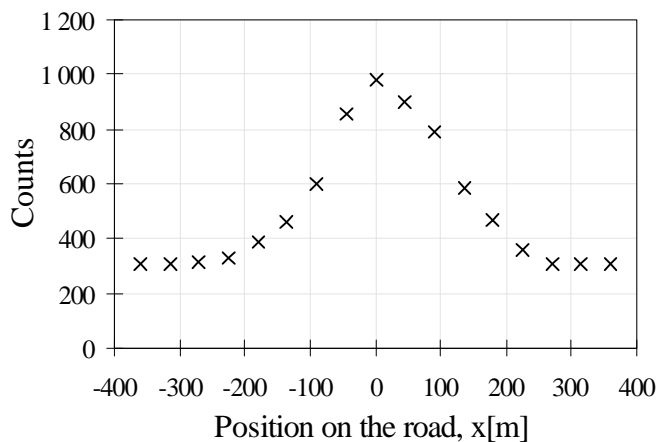


**Fig 3.3.** Counts in the Cs window for 32 km/h, detector backwards. The source placed 100 m from the road.

This data is now analysed with the method explained in section 2.2.1 and the  $t$ -test.

The results is then:

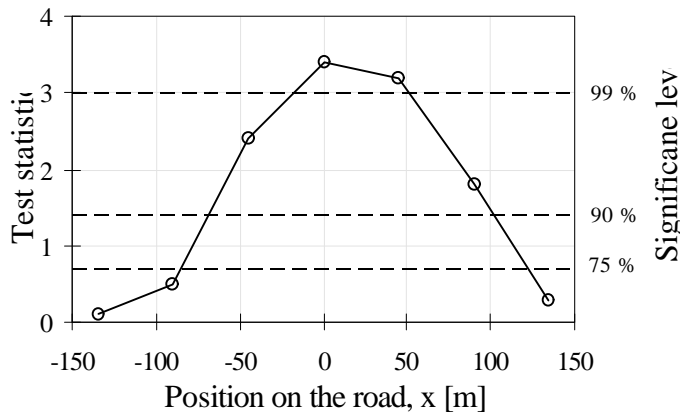


**Fig 3.4.** The results of the  $t$ -test for 32 km/h, detector backwards. The source placed 100 m from the road.

Same procedure was performed for the three other source-road distances.

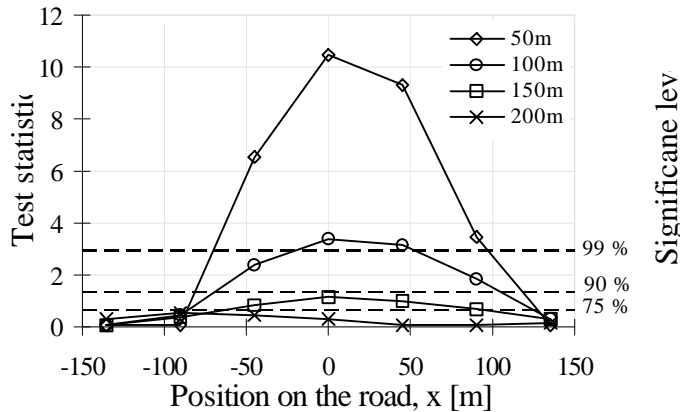


**Fig 3.5.** The results of the  $t$ -test for 32 km/h, detector directed backwards.

It is now time to decide the significance level. It should be set as low as possible to minimise the risk for missing a source, but high enough to avoid an unacceptable frequency of false alarms caused by variations in the background radiation. Field measurements on the short term spatial variations in the background radiation are to be performed to determine the amount of false alarms at a given significance level. In this report the 90% significance level will be used as more of an example than a recommendation.

Now when the level is chosen one sees in figure 3.5 that the detection limit is between 100 m and 150 m. If the highest  $t$  value for each source-road distance are plotted as a function of source-road distance an exponential curve can be fitted to the data. From this the detection limit can be determined.

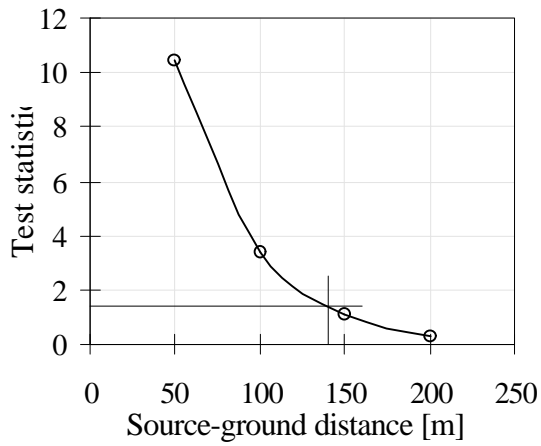


**Fig 3.6.** Determination of the detection limit for 32 km/h, detector directed backwards. The detection limit is the source-ground distance corresponding to  $t=1,42$ . In this case approximately 140 m.

From figure 3.6 the detection limit, for 32 km/h and the detector in the backward geometry, is determined to 140 m. Same procedure for the other speeds and geometries gives:

Speed	Backwards	Sideways “wrong side”	Sideways “right side”
32 km/h	140 m	160 m	190 m
54 km/h	160 m	180 m	210 m
68 km/h	160 m	180 m	210 m

**Fig 3.7.** Detection limits for the three speeds and the three geometries

## 4. Discussion

### 4.1 Geometry

The detection limit is about 30 to 35 % better in the sideward geometry if the source lies on the same side as the crystal is directed, compared to the backward geometry, figure 3.7. This is, as mentioned earlier, due to the physical dimensions of the crystal. The projected area from the front and from the side of the detector has a ratio of roughly 5:3. This ratio leads to that about 50 - 70 % more pulses are recorded in the Cs window for the sideward (“right side”) geometry.

The other notation in figure 3.7 is that the detection limit is about 10 to 15 % better when the PM-tubes are facing the source compared to the backward geometry. The reason for this is that the attenuating effect of the PM-tubes for 662 keV photons is less important than the direction of the crystal. These two properties lead to the recommendation of placing the crystal in the sideways direction, for a  $^{137}\text{Cs}$  source. If the source had been low energetic, *e.g.*  $^{99}\text{Tc}^m$ , the result might have been different, due to the increased attenuation in the PM-tubes.

### 4.2 The detection limit calculation method

One, at first sight, surprisingly feature about the result is that the detection limit is lowest for the slowest speed. Intuitive it should be easier to find a source if the car moves slower. The reason why the detection limit is lower when the car is going slower is because it is a strong source at a large distance. Which means that the source contributes to a peak in several consecutive spectra; the slower you drive the more spectra is influenced by the source. It is easy to explain why the method that compares nine consecutive spectra do not work at low speeds by an example:

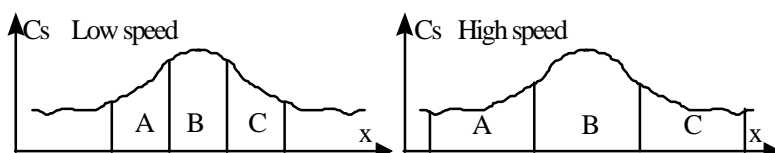


*Fig 4.1.* Schematic picture of the count rate in the Cs window change as a function of the co-ordinate on the road for a strong source at large distance .

The areas marked A to C in figure 4.1 represents the counts in the six surrounding spectra (A,C) and the three in the middle (B). The test checks the value of  $B - \frac{1}{2}(A+C)$ ;

it is then obviously that this value is lower in the case with low speed. If this is drawn to it's extreme, we let the speed reaching zero,  $B - \frac{1}{2}(A+C) = 0$ ; the test do not see the source at all. The detection limit has also been calculated for the best possible geometry for 90 km/h, the result was then 200 m, which is lower then for 68 km/h. The optimal speed with this analysis method the measurements at Revingehed seems to be about 70 km/h.

The method of analysis might on the other hand be useful for searching for sources that only contributes to pulses in three or less consecutive spectra, *i.e.* a weak source that is lying near the road or a collimated strong source far from the road. The surrounding spectra will then only consist of background: The problem above with photons from the source in the surrounding spectra is then negligible.

### **4.3 Conclusions**

The method studied in this report is not a general one for finding point sources. It is an easy and probably useful method for finding weak sources near the road but it is not the best method for finding strong sources far away from the road, unless they are collimated.

A more general conclusion is that the detector should be placed so that the crystal is facing one side of the road, if the search is for a source with energy of the same order as  $^{137}\text{Cs}$  and using a full energy peak window as base for the analysis.

A recommendation regarding the speed of the car is yet to be investigated. It is hard to draw any reliable conclusions from the work in this report due to the lack of generality of the method studied.

During ideal circumstances, driving in 70 km/h and the crystal directed at the right side, the 6 GBq  $^{137}\text{Cs}$  source can be detected 210 m from the road with the analysis method used in this report.

### **4.4 Further studies**

There is a lot to be done in the developing of methods for finding lost point sources. The first step is to test other methods for analysing the data obtained at Revingehed. An interesting approach is to involve, somehow, the shape of the curve in figure 3.3

The curve is plotted again, now with the corresponding curves for the two larger distances:

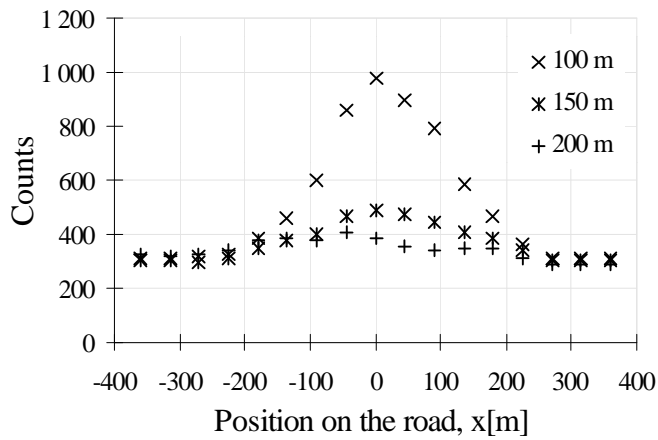


**Fig 4.2.** Counts in the Cs window for 32 km/h, detector backwards. The source placed 100, 150 and 200 m from the road.

Above was the detection limit calculated to 140 m for this geometry and speed. In the curve for the source-road distance 150 m a clear symmetrical bump around x equal zero is present. Maybe this could be the cause of natural background. A method could hopefully be found that reacts not at the small increase in pulses compared to surrounding spectra but on the smooth symmetrical shape of the curve.

Another step to do is to evaluate data obtained for sources with different energies, data is already collected at Revingehed for  $^{99}\text{Tc}^m$  and  $^{131}\text{I}$ .

## **Acknowledgements**

I will thank following people for making this project possible:

My supervisors Christer Samuelsson and Jacob Eberhardt for sharing there knowledge and contributing with ideas.

Robert Finck and Hans Mellander, SSI, whom without the project would not exist.

Special thanks to Robert for all the help with the field measurements at Revingehed.

Lars Upphed, SSI, for the arrangements with the transportation of the Cs-source.

Lennart Bergqvist, Radionuklidcentralen Lund.

The military personnel at P7 Revingehed for the good co-operation.

Finally, of course, SSI for the economical support.

## References

1. *Bristow, Q, Current Research, Part B, Geological Survey of Canada Paper78-1B, 1978, **The application of Airborne Gamma Ray Spectrometry in the search for Radio Active Debris from the Russian Satellite Cosmos 954 (Operation Morning Light).***
2. *Deal, L.J, Doyle, J.F., Burson, Z.G., Boyns, P.K., Health Physics, vol. 23, Pergamon Press, Oxford, 1972. **Locating the lost Athena Missile in Mexico by the Aerial Radiological Measuring System (ARMS).***
3. *Finck R, Swedish Radiation Protection Institute,1996. **Personal communication***
4. *Grasty, R.L, Search theory and applications, Plenum press, London and New York, 1979, **The search for Cosmos 954.***
5. *IAEA , Technical reports series no. 186, 1979, **Gamma-Ray Surveys in Uranium Exploration.***
6. *IAEA , Technical reports series no. 323, 1991, **Airborne Gamma Ray Spectrometer Surveying.***
7. *Knoll G.F, John Wiley & Sons, 1989, **Radiation Detection and Measurement***
8. *Mellander H, Swedish Geological Co. Report TFRAP 8803 ,1988, **Airborne Gammaspectrometric Measurements of the Fall-out over Sweden after the Nuclear Reactor Accident in Chernobyl, USSR.***
9. *Samuelsson C, Eberhardt J, unpublished. **Result from the NKS organised exercise RESUMÉ in Finland 1995.***
10. *SGAB, Swedish Geological Co. Report TFRAP 9005 ,1990, **Technical Report about the Air Borne Gamma Ray Survey performed in Sweden after the Chernobyl Accident .***

## From raw data to results

This appendix presents in detail how the spectra used in the calculation of the detection limit were constructed from the primary measurements. The approach for the analysis was to measure with the car standing still on the road instead of driving, and then theoretically estimate the spectra that would be obtained at mobile measurements.

### Data collection

The optimal place for the measurements would be a very large open space with small changes in the natural background. Through the area a straight road should run, at least 1000 m long. A place with almost all of the above features were found; the military training ground at Revingehed, Skåne. There was only one thing this field could not offer, a long road enough. Therefore the source was placed as follows:

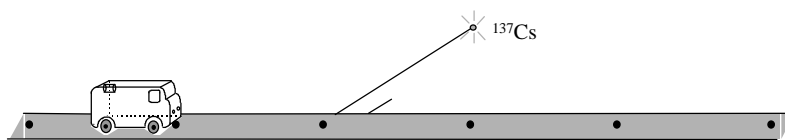


**Fig A.1.** The optimal area.

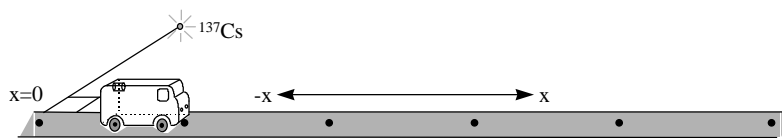


**Fig A.2.** Where the measurements were performed at Revingehed.

The measuring points were located 25 m apart, the first were located at the point on the road that was closest to the source ( $x=0$ ). Measurements at 12 points were performed, *i.e.* the last point was 275 m from the first point. At each of these points the following source-road distances 50, 100, 150 and 200 m were measured:

- 1) 30 s spectra, detector backwards, car pointing in x direction.
- 2) 30 s spectra, detector backwards, car pointing in -x direction.
- 3) 30 s spectra, detector sideways, car pointing in x direction.
- 4) 30 s spectra, detector sideways, car pointing in -x direction.
- 5) 5 min background spectra, detector backwards
- 6) 5 min background spectra, detector sideways, car pointing in x direction.
- 7) 5 min background spectra, detector sideways, car pointing in -x direction.

The background was assumed to be the same in both car directions for the detector geometry pointing backwards.

Next step was to create full sets of data, that is create the spectra that would be obtained at negative  $x$  (left of the source in figure A.2). Collected data were “mirrored” to the left side of the source. The spectra in measurements 2) above were used as the spectra that would have been obtained left of the source in an optimal area when the car is pointing in  $x$  direction. To get the spectra left of the source for 3) and 4) it was simply assumed that the spectra were symmetrical around  $x = 0$ .

Thus, spectra from  $x = -275$  m to  $x = 275$  m have been constructed.

### **Interpolation to 5 m apart**

The parameter of interest is what the total counts in the Cs window, 500 to 800 keV, would be in spectra collected when driving. The first step towards this is to calculate the count rate in that energy interval every 5 meters on the road from the measured spectra. The following procedure were performed on the spectra:

- 1) Energy calibration on the  $^{137}\text{Cs}$  and  $^{40}\text{K}$  peaks.
- 2) Division with the live time to obtain count rates.
- 3) Transforming the spectra to the same energy width, 12,5 keV/ch. This were done by multiplying the count rate in all channels with the factor  $x/12,5$ , where  $x$  is the original energy width.
- 4) Linear interpolation to get the cps in  $E = 500, 512,5, 525, \dots, 800$  keV.
- 5) Subtraction of the background in the Cs window (this is done so interpolation of the count rate from the source between the measuring points is possible).
- 6) The net count rate in the Cs window,  $N_{Cs,net}$ , is calculated.
- 7)  $N_{Cs,net}$  is corrected for attenuation in the air and the inverse square law (to make linear interpolation of  $N_{Cs,net}$  between the measuring points possible).
- 8) The corrected count rate,  $N_{Cs,net*}$ , is then linear interpolated to  $x = 5, 10, 15, 20, 30, 35, \dots, 270$  m.
- 9) The corrections in 7) are now done inverted on all the data and the background is added back.

After this long procedure we finally have the total count rates in the Cs window every 5 meters on the road for the three detector geometries and four source-detector distances.

### **Sampling**

The final step is to construct spectra at different speeds from the calculated Cs window count rates. The speeds used was 9, 15 and 19 m/s and the sampling time was 5 s. The procedure for 9 m/s is presented, all the others are constructed the same way.

In 5 s at the speed of 9 m/s the car drives 45 m, i.e. the car passes 15 of the points where the count rate is calculated. The total counts in the Cs window,  $N_{Cs}$ , is then estimated by:

$$N_{Cs} = 5/15(N_{Cs,1} + N_{Cs,2} + N_{Cs,3} + \dots + N_{Cs,15})$$

where  $N_{Cs,i}$  is the above calculated count rates in the Cs window. The co-ordinate on the road for the sampled spectrum is set to the middle one, in this case the co-ordinate for  $N_{Cs,8}$ .

## Data on the $\mu$ ACE™ amplifier and MCA card

### Hardware specifications

**Amplifier Input** Accepts input from the charge sensitive preamplifier in the EG&G ORTEC ScintiPack PMT Base and Bias Supply. Other external signals must be positive with rise times  $<0.1 \mu\text{s}$  and decay times  $>40 \mu\text{s}$ .

$Z_{\text{in}} = 1000 \Omega$ , ac-coupled. Linear maximum input = 5 V.

**Amplifier Output** Linear bipolar pulse, 0 to 2 V in amplitude, 3.5  $\mu\text{s}$  peaking time.

$Z_{\text{out}} = 825 \Omega$ .

**Amplifier Gain** Variable from 5 to 25 under computer control, with resolution one part in 4096.

**Amplifier Pulse Shape** Peaking time equals 3.5  $\mu\text{s}$  and is semi-Gaussian bipolar.

**External Input** Accepts positive unipolar or positive leading bipolar analog pulses with peaking times from 2 to 20  $\mu\text{s}$ .  $Z_{\text{in}} = 1000 \Omega$ , dc-coupled. Linear maximum input 10 V, absolute maximum input 20 V.

**Pulse-Height Analysis** Wilkinson type ADC with 512- or 2048-channel conversion gain selectable by printed wiring board (PWB) jumpers. Factory set for 512 channels. The conversion gain can be set via software to 256 or 512 with the jumper in the 512 position, and to 256, 512, 1024, or 2048 with the jumper in the 2048 position.

**Conversion Time**  $<7 \mu\text{s}$  for 512-channel resolution;  $<30 \mu\text{s}$  for 2048-channel resolution. 80-MHz clock.

**Data Memory** 2048 channels,  $2^{31} - 1$  counts per channel.

**Dead-Time Correction** Gedcke-Hale Method.

**Integral Nonlinearity**  $<0.1\%$  over 98% dynamic range.

**Differential Nonlinearity**  $<2\%$  over 98% of full scale.

**Spectrum Broadening** Typically  $<3\%$  broadening at FWHM, for 0 to 100 000 counts per second, on the 661 keV  $^{137}\text{Cs}$ - line, using an EG&G ORTEC ScintiPack PMT Base and Model 905-4 NaI detector.

**Spectrum Shift** (Stabilizer inactive) Typically  $<\pm 3\%$  for 0 to 100 000 counts per second, on the 661 keV  $^{137}\text{Cs}$  line, using an EG&G ORTEC ScintiPack PMT Base and Model 905-4 NaI detector.

**Presets**

**Real Time/Live Time** In multiples of 20 ms.

**Region-Of-Interest** Peak or integral counts.

**Data Overflow** Terminates when the data in any channel exceeds  $2^{31} - 1$  counts.

**Connectors**

**IN/OUT** Rear-panel BNC connector. The PWB jumper selects either the output of the internal amplifier or external input to the ADC. When internal amplifier is selected, the connector can be used as a monitor for the shaping amplifier output. When the external input is selected, the connector allows an external amplifier to be used with the ADC.

**GATE** Rear-panel BNC connector for optional slow positive NIM input, coincidence or anticoincidence; must occur prior to and extend beyond 0.5  $\mu$ s from ADC peak detect. Software selectable as OFF/COIN/ANTI.

**Preamp Power** Rear-panel 9-pin D connector provides +12 V power to the ScintiPack PMT Base and provides the energy signal from the preamplifier to the internal shaping amplifier via pin 3.

**Controls**

**LLD** Rear-panel screwdriver potentiometer, 0 to 20% of full scale.

**ZERO** Rear-panel screwdriver potentiometer,  $\pm 4\%$  of full scale.

**Electrical and mechanical**

**Dimensions** 17.8 cm (7 in.) X 10.8 cm (4.25 in.).

**Power Required** 1.5 Watts; +5 V, 250 mA; - 5 V, 50 mA; (+12 V, 20 mA, for operation of the ScintiPack PMT Base and Bias Supply).

**Slot Requirement** IBM PC standard card, 2/3 slot required. Up to 8 cards may be controlled by a single PC, space permitting.